THEORETICAL AND APPLIED MECHANICS
Volume 48 (2021) Issue 2, 237–255 DOI: https://doi.org/10.2298/TAM200923010K

A MIXED BOUNDARY VALUE PROBLEM OF A CRACKED ELASTIC MEDIUM UNDER TORSION

Belkacem Kebli and Fateh Madani

Abstract. The present work aims to investigate a penny-shaped crack problem in the interior of a homogeneous elastic material under axisymmetric torsion by a circular rigid inclusion embedded in the elastic medium. With the use of the Hankel integral transformation method, the mixed boundary value problem is reduced to a system of dual integral equations. The latter is converted into a regular system of Fredholm integral equations of the second kind which is then solved by quadrature rule. Numerical results for the displacement, stress and stress intensity factor are presented graphically in some particular cases of the problem.

1. Introduction

The category of problems which concerns the state of stresses and displacements in an elastic layer medium, due to the torsion of a circular inclusion in bonded contact, has been a subject of much interest in geotechnical engineering, civil engineering and applied mechanics. It may give a better understanding of the behavior of foundations under external loads. In structure-medium interaction problems arising in foundation engineering, the foundation is usually modeled using a rigid or flexible inclusion having a circular, strip, rectangular or arbitrary shape. Generally, an inclusion in contact with an elastic medium can be excited by normal translation, lateral translation, rocking rotation and torsional rotation. From a practical viewpoint, in geomechanical applications, the inclusion may represent the resinous or cementing material, which is used to transfer the anchoring loads to the geological medium [1]. In this category of problems the penny-shaped crack can be caused by thermally induced stresses in the dilatation of the inclusion or the hydraulic fracture.

It has been shown that for foundations in which the depth of embedment exceeds the dimension of the foundation by ten times, the medium can be considered as infinite elastic space [2]. For the case of infinite embedment of the rigid disc in an

2010 *Mathematics Subject Classification:* 33C10; 34B60; 41A55; 44A05; 45B05.

Key words and phrases: elastic medium, axisymmetric torsion, penny-shaped crack, dual integral equations, Fredholm integral equations, stress intensity factor.

infinite elastic solid (deeply embedded), Selvadurai [3,4] investigated the asymmetric contact problems related to a rigid circular inclusion disc embedded in bonded contact with an isotropic elastic medium. Their results depend on the rotational or translational stiffnesses for the embedded rigid circular disc. The problem of the torsion of an elastic half space was first considered by Reissner and Sagoci [5]. They studied the static interaction of a rigid disc and an elastic isotropic half-space for which they obtained the solution by means of the spheroidal coordinates. Sneddon [6, 7] re-studied the classical Reissner–Sagoci problem using the Hankel transforms method for reduction of the problem to a pair of dual integral equations. Ufliand [8] set up the dual integral equations for the Reissner–Sagoci problem for a circular disc on an elastic layer and reduced them to the solution of a Fredholm integral equation of the second kind. Collins [9] treated the torsional problem of an elastic half-space by supposing the displacement at any point in the half-space to be due to a distribution of wave sources over the part of the free surface in contact with the disc. The solution for the forced vibration problem of an elastic layer of finite thickness when the lower face is either stress free or rigidly clamped was given by Gladwell [10], who reduced the mixed boundary value problem to a Fredholm integral equation by Noble's method [11]. Singh and Dhaliwal [12] investigated the Reissner–Sagoci problem for an elastic layer under torsion by a pair of circular discs on opposite faces. The Reissner–Sagoci problem with a rigid circular punch bound to the surface of a transversely isotropic elastic half-space was solved by Selvadurai [13]. Pak and Saphores [14] provided an analytical formulation for the general colortorsional problem of a rigid disc embedded in an isotropic half-space. The quadrature numerical was used for solving the obtained Fredholm integral equation. Besides, Bacci and Bennati [15] employed the Hankel transforms method and the power series method with the truncation of the second term to consider the torsion of a circular rigid disc adhered to the upper surface of an elastic layer fixed to an undeformable support. More recently, Singh et al. [16] studied the static torsional loading of a non-homogeneous, isotropic, half-space by rotating a circular part of its boundary surface. The solution for the corresponding triple integral equations was reduced to the solution for two simultaneous integral equations. Cai and Zue [17] discussed the torsional vibration of a rigid disc bonded to a poro-elastic multilayered medium. They used the Hankel transforms and transferring matrix method. Rahimian [18] et al. studied the problem of torsion in a transversely isotropic half-space by a rigid circular disc. Using a cylindrical co-ordinate system and applying the Hankel integral transform in the radial direction, the problem may be changed to a system of dual integral equations. Yu [19] studied the forced torsional oscillations inside the multilayered solid. Elastodynamic Green's function of the center of rotation and a point load method were used to solve the problem. Pal and Mandal [20] considered the forced torsional oscillations of a transversely isotropic elastic half-space under the action of an inside rigid disc. The studied problem was transformed to a dual integral equations system which was reduced to a Fredholm integral equation. A similar problem with the rocking rotation was solved later on by Ahmadi and Eskandari [21]. They used appropriate Green's function to write the mixed boundary-value problem posed as a dual integral equation.

The torsional problem of elastic layers with a penny shaped crack was considered by some researchers. Sih and Chen [22] studied the problem of a penny-shaped crack in a layered composite under a uniform torsional stress. The displacement and stress fields throughout the composite were obtained by solving a standard Fredholm integral equation of the second kind. Low [23] investigated a problem of the effects of embedded flaws in the form of an inclusion or a crack in an elastic half-space subjected to torsional deformations. The corresponding Fredholm integral equations were solved numerically by quadrature approach. The same method was used by Dhawan [24] for solving the problem of a rigid disc attached to an elastic half-space with an internal crack. By using Hankel and Laplace transforms and taking numerical inversion of the Laplace transform, Basu and Mandal [25] treated the torsional load on a penny-shaped crack in an elastic layer sandwiched between two elastic half-spaces. With the aid of the Hankel integral transformation method, in this paper we investigate the problem of a penny-shaped crack in the interior of a homogeneous elastic medium under axisymmetric torsion applied to a rigid disc glued inside. The mixed boundary-value problem is written as a system of dual integral equations. The corresponding system of Fredholm integral equations was approached by sets of linear equations. After getting the unknown coefficients of this system we obtain numerical results and display curves according to certain pertinent parameters.

2. Formulation of the problem

We consider the axisymmetric torsion of a circular rigid inclusion of a radius b situated on a plane $z = h$ in an infinite, isotropic and homogeneous elastic medium, containing a penny-shaped crack in the region $0 < r < a$, $z = 0$. The faces of the crack are supposed to be stress free while the rigid circular disc inclusion rotates with an angle ω about the z axis passing through their centers as shown in Figure 1.

As the studied configuration is axisymmetric and the loading (radially symmetric) where the angular displacement u_θ depends only on r and z, then the radial and axial displacement components are zero, that is, $u_r = u_z = 0$.

Then the only non-zero components stresses are related to the displacement component by

$$\tau_{\theta z} = G\frac{\partial u_\theta}{\partial z}, \qquad \tau_{\theta r} = Gr\frac{\partial}{\partial r}\Big(\frac{u_\theta}{r}\Big), \tag{2.1}$$

where G is the shear modulus of the material.

For the static axisymmetric torsion of a homogeneous isotropic material and linear elastic behavior, the displacement satisfies the following differential equation

$$\frac{\partial^2 u_\theta}{\partial r^2} + \frac{\partial u_\theta}{r\partial r} - \frac{u_\theta}{r^2} + \frac{\partial^2 u_\theta}{\partial z^2} = 0. \tag{2.2}$$

By applying the Hankel integral transform from [26] to (2.2)

$$F(\lambda, z) = \int_0^\infty f(r, z) r J_1(\lambda r) dr, \tag{2.3}$$

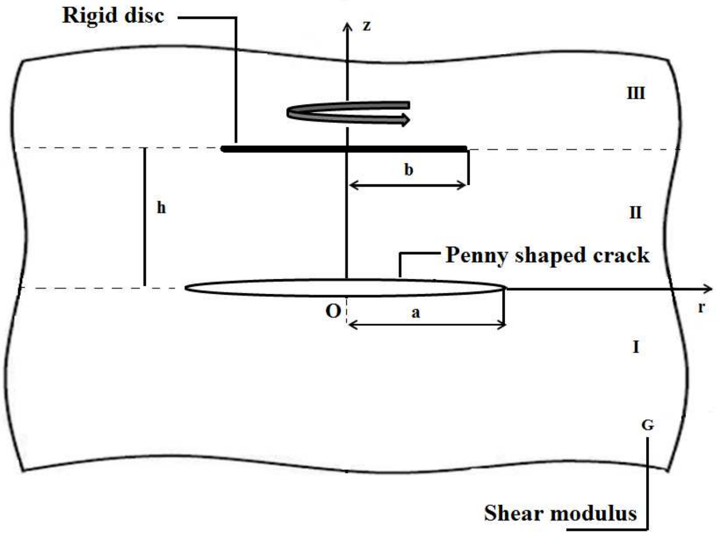

Figure 1. Geometry and coordinate system

and the Hankel inversion transform

$$f(r,z)=\int_0^\infty F(\lambda,z)\lambda J_1(\lambda r)d\lambda, \tag{2.4}$$

where J_1 is the Bessel function of the first kind of order one, we find the general solution for Eq. (2.2) for the regions I ($z\leqslant 0$), II ($0\leqslant z\leqslant h$) and III ($z\geqslant h$) as shown in Figure 1 as

$$u_\theta^{(i)}(r,z)=\int_0^\infty [A_i(\lambda)e^{-\lambda z}+B_i(\lambda)e^{\lambda z}]J_1(\lambda r)d\lambda,\quad i=1,2,3, \tag{2.5}$$

where A_i and B_i are unknown functions.

3. Boundary and continuity conditions

Let us assume the contact between the rigid circular inclusion and the elastic layer is perfectly bonded all along their common interface. We consider the regularity conditions at infinity, the boundary and continuity conditions at $z=h$, as shown below.

At infinity, the regularity conditions are given by

$$\lim_{|z|\to\infty} u_\theta(r,z)=0,\qquad \lim_{|z|\to\infty}\tau_{\theta z}(r,z)=0. \tag{3.1}$$

The boundary conditions of the problem are

$$\tau_{\theta z}^{(2)}(r,0^+)=\tau_{\theta z}^{(1)}(r,0^-)=0,\quad r<a, \tag{3.2a}$$

$$u_\theta^{(3)}(r,h)=u_\theta^{(2)}(r,h)=\omega r,\quad r\leqslant b. \tag{3.2b}$$

The continuity conditions of the problem in the planes $z=0$ and $z=h$ can be written as

$$u_\theta^{(2)}(r,0^+)-u_\theta^{(1)}(r,0^-)=0,\quad r\geqslant a, \tag{3.3a}$$

$$\tau_{\theta z}^{(2)}(r,0^+)-\tau_{\theta z}^{(1)}(r,0^-)=0,\quad r\geqslant a, \tag{3.3b}$$

$$u_\theta^{(3)}(r,h^+)-u_\theta^{(2)}(r,h^-)=0,\quad r>b, \tag{3.3c}$$

$$\tau_{\theta z}^{(3)}(r,h^+)-\tau_{\theta z}^{(2)}(r,h^-)=0,\quad r>b. \tag{3.3d}$$

By utilizing the condition expressed by Eq. (3.1), the expressions of displacements and stresses in the three regions take the following forms

$$u_\theta^{(1)}(r,z)=\int_0^\infty B_1(\lambda)e^{\lambda z}J_1(\lambda r)d\lambda, \tag{3.4a}$$

$$\tau_{\theta z}^{(1)}(r,z)=G\int_0^\infty \lambda B_1(\lambda)e^{\lambda z}J_1(\lambda r)d\lambda, \tag{3.4b}$$

$$u_\theta^{(2)}(r,z)=\int_0^\infty [A_2(\lambda)e^{-\lambda z}+B_2(\lambda)e^{\lambda z}]J_1(\lambda r)d\lambda, \tag{3.4c}$$

$$\tau_{\theta z}^{(2)}(r,z)=G\int_0^\infty \lambda[-A_2(\lambda)e^{-\lambda z}+B_2(\lambda)e^{\lambda z}]J_1(\lambda r)d\lambda, \tag{3.4d}$$

$$u_\theta^{(3)}(r,z)=\int_0^\infty A_3(\lambda)e^{-\lambda z}J_1(\lambda r)d\lambda, \tag{3.4e}$$

$$\tau_{\theta z}^{(3)}(r,z)=-G\int_0^\infty \lambda A_3(\lambda)e^{-\lambda z}J_1(\lambda r)d\lambda. \tag{3.4f}$$

The unknown functions $B_1(\lambda)$, $A_2(\lambda)$, $B_2(\lambda)$ and $A_3(\lambda)$ can be determined from the boundary and continuity conditions.

The boundary and continuity conditions expressed by Eqs. (3.2a), (3.3b), (3.2b) and (3.3c) show that

$$\tau_{\theta z}^{(2)}(r,0^+)-\tau_{\theta z}^{(1)}(r,0^-)=0,\quad r\geqslant 0, \tag{3.5a}$$

$$u_\theta^{(3)}(r,h^+)-u_\theta^{(2)}(r,h^-)=0,\quad r\geqslant 0. \tag{3.5b}$$

The continuity conditions expressed by Eqs. (3.3b) and (3.3c) lead to

$$B_1(\lambda)=B_2(\lambda)-A_2(\lambda), \tag{3.6a}$$

$$A_3(\lambda)=B_2(\lambda)e^{2\lambda h}+A_2(\lambda). \tag{3.6b}$$

From the mixed boundary conditions expressed by Eqs. (3.2a), (3.3a), (3.2b) and (3.3d), we find the system of dual integral equations for obtaining the unknown functions A_2 and B_2

$$\int_0^\infty \lambda[B_2(\lambda)-A_2(\lambda)]J_1(\lambda r)d\lambda=0,\quad r<a, \tag{3.7a}$$

$$\int_0^\infty A_2(\lambda)J_1(\lambda r)d\lambda = 0, \quad r \geqslant a, \tag{3.7b}$$

$$\int_0^\infty [A_2(\lambda)e^{-\lambda h} + B_2(\lambda)e^{\lambda h}]J_1(\lambda r)d\lambda = \omega r, \quad r \leqslant b, \tag{3.7c}$$

$$\int_0^\infty \lambda B_2(\lambda)e^{\lambda h}J_1(\lambda r)d\lambda = 0, \quad r > b. \tag{3.7d}$$

3.1. Limiting cases. By taking the limit $a \to \infty$, the problem is simplified to the torsional rotation of a rigid cirular inclusion in a homogeneous elastic half-space, and the dual integral equations become:

$$\int_0^\infty [A_2(\lambda)e^{-\lambda h} + B_2(\lambda)e^{\lambda h}]J_1(\lambda r)d\lambda = \omega r, \quad r \leqslant b, \tag{3.8a}$$

$$\int_0^\infty \lambda B_2(\lambda)e^{\lambda h}J_1(\lambda r)d\lambda = 0, \quad r > b. \tag{3.8b}$$

This pair of dual integral equations has the same meaning as (18a) and (18b) in Pak's paper [14].

Let us take the limit $a \to 0$. Then one can obtain the closed-form solution pertinent to the torsional rotation of a rigid disc embedded in a homogeneous elastic full-space. Due to the symmetry of the full-space case with respect to the plane of the disc, it can be deduced that $\tau_\theta z$ is zero for $r > a$ at the disc plane. This situation corresponds exactly to the torsion of a homogeneous elastic half-space by a circular rigid disc $(0 < r < a, z = 0)$ bonded to the surface. This is adapted to the problem concerning the isotropic half-space considered by Reissner and Sagoci [5].

4. Reduction of the problem to a system of Fredholm integral equations

The system of dual equations can be reduced to a system of Fredholm integral equations of the second kind by introducing the auxiliary functions $\phi(t)$ and $\psi(t)$ such that

$$A_2(\lambda) = \sqrt{\lambda}\int_0^a \sqrt{t}\phi(t)J_{\frac{3}{2}}(\lambda t)dt, \tag{4.1a}$$

$$B_2(\lambda) = e^{-\lambda h}\sqrt{\lambda}\int_0^b \sqrt{t}\psi(t)J_{\frac{1}{2}}(\lambda t)dt. \tag{4.1b}$$

With this choice of the new unknown functions, we find that the homogeneous Equations (3.7b) and (3.7d) are identically satisfied while Equations (3.7a) and (3.7c) lead to Fredholm's integral equations.

By inserting $A_2(\lambda)$ and $B_2(\lambda)$ in the Equations (3.7a) and Eq. (3.7c), we get

$$\begin{aligned}\int_0^a \sqrt{t}\phi(t)dt\int_0^\infty \lambda^{\frac{3}{2}}J_{\frac{3}{2}}(\lambda t)J_1(\lambda r)d\lambda \\ - \int_0^b \sqrt{t}\psi(t)dt\int_0^\infty \lambda^{\frac{3}{2}}e^{-\lambda h}J_{\frac{1}{2}}(\lambda t)J_1(\lambda r)d\lambda = 0, \quad r < a,\end{aligned} \tag{4.2}$$

$$(4.3)\quad \int_0^a \sqrt{t}\phi(t)dt \int_0^\infty \sqrt{\lambda} e^{-\lambda h} J_{\frac{3}{2}}(\lambda t) J_1(\lambda r) d\lambda \\ + \int_0^b \sqrt{t}\psi(t)dt \int_0^\infty \sqrt{\lambda} J_{\frac{1}{2}}(\lambda t) J_1(\lambda r) d\lambda = \omega r, \quad r < b.$$

To find the first Fredholm integral equation, we use $\lambda J_1(\lambda r) = \frac{1}{r^2}\frac{d}{dr}[r^2 J_2(\lambda r)]$ and taking into account the integral formula

$$(4.4)\quad \int_0^\infty \sqrt{\lambda} J_{\frac{3}{2}}(\lambda t) J_2(\lambda r) d\lambda = \begin{cases} \sqrt{\frac{2}{\pi}} \frac{t^{\frac{3}{2}}}{r^2\sqrt{r^2-t^2}} & t < r \\ 0 & t > r \end{cases},$$

we obtain the Abel equation corresponding to Eq. (4.2)

$$(4.5)\quad \sqrt{\frac{2}{\pi}} \int_0^r \frac{t^2\phi(t)}{\sqrt{r^2-t^2}} dt - r^2 \int_0^b \sqrt{t}\psi(t)dt \\ \int_0^\infty \sqrt{\lambda} e^{-\lambda h} J_{\frac{1}{2}}(\lambda t) J_2(\lambda r) d\lambda = 0, \quad r < a.$$

By applying Abel's transform formula

$$(4.6)\quad \int_0^r \frac{f(t)}{\sqrt{r^2-t^2}} dt = g(r) \quad \text{then} \quad f(t) = \frac{2}{\pi}\frac{d}{dt}\int_0^t \frac{r g(r)}{\sqrt{t^2-r^2}} dr,$$

we find from Eq. (4.5) that

$$(4.7)\quad t^2\phi(t) = \sqrt{\frac{2}{\pi}} \frac{d}{dt} \int_0^t \frac{r^3}{\sqrt{t^2-r^2}} \Bigg[\int_0^b \sqrt{\delta}\psi(\delta) d\delta \\ \int_0^\infty \sqrt{\lambda} e^{-\lambda h} J_{\frac{1}{2}}(\lambda\delta) J_2(\lambda r) d\lambda \Bigg] dr, \quad r < a.$$

For the right hand side of the above equation, the integral is further simplified by using the following relationship

$$(4.8)\quad \sqrt{\frac{2}{\pi}} \frac{d}{dt} \int_0^t \frac{r^3}{\sqrt{t^2-r^2}} J_2(\lambda r) dr = \sqrt{\lambda} t^{\frac{5}{2}} J_{\frac{3}{2}}(\lambda t),$$

and we obtain the first Fredholm integral equation of the second kind

$$(4.9)\quad \phi(t) + \sqrt{t} \int_0^b \sqrt{\delta}\psi(\delta) K(t,\delta) d\delta = 0, \quad r < a,$$

where

$$K(t,\delta) = -\int_0^\infty \lambda e^{-\lambda h} J_{\frac{3}{2}}(\lambda t) J_{\frac{1}{2}}(\lambda\delta) d\lambda.$$

Similarly, Eq. (4.3) can be reduced to the second Fredholm integral equation by using the formula

$$(4.10)\quad \int_0^\infty \sqrt{\lambda} J_{\frac{1}{2}}(\lambda t) J_1(\lambda r) d\lambda = \begin{cases} \sqrt{\frac{2t}{\pi}} \frac{1}{r\sqrt{r^2-t^2}}, & t < r \\ 0, & t > r \end{cases},$$

and we obtain the following Abel equation

$$(4.11)\quad \frac{1}{r}\sqrt{\frac{2}{\pi}}\int_0^r \frac{t\psi(t)}{\sqrt{r^2-t^2}}dt+\int_0^a \sqrt{t}\phi(t)dt \int_0^\infty \sqrt{\lambda}e^{-\lambda h}J_{\frac{3}{2}}(\lambda t)J_1(\lambda r)d\lambda=\omega r,\quad r<b.$$

By applying the Abel's transform formula to the last equation, we obtain

$$(4.12)\quad t\psi(t)=\sqrt{\frac{2}{\pi}}\frac{d}{dt}\int_0^t \frac{r^2}{\sqrt{t^2-r^2}}\Big[\omega r-\int_0^a\sqrt{\delta}\phi(\delta)d\delta \int_0^\infty \sqrt{\lambda}e^{-\lambda h}J_{\frac{3}{2}}(\lambda\delta)J_1(\lambda r)d\lambda\Big]dr,\quad r<b.$$

Using the following relationship

$$(4.13)\quad \frac{d}{dt}\int_0^t \frac{r^3}{\sqrt{t^2-r^2}}dr=2t^2,$$

$$(4.14)\quad \sqrt{\frac{2}{\pi}}\frac{d}{dt}\int_0^t \frac{r^2J_1(\lambda r)}{\sqrt{t^2-r^2}}dr=t\sqrt{\lambda t}J_{\frac{1}{2}}(\lambda t),$$

we finally get the second Fredholm integral equation of the second kind

$$(4.15)\quad \psi(t)+\sqrt{t}\int_0^a\sqrt{\delta}\phi(\delta)L(t,\delta)d\delta=\frac{4\omega}{\sqrt{2\pi}}t,\quad t<b,$$

with the kernel

$$L(t,\delta)=\int_0^\infty \lambda e^{-\lambda h}J_{\frac{1}{2}}(\lambda t)J_{\frac{3}{2}}(\lambda\delta)d\lambda.$$

The system given by Eq. (4.9) and Eq. (4.15) can be written in the dimensionless form as follows.

We put

$$(4.16)\quad \begin{cases}\delta=a\eta, & 0<\delta<a; \quad t=a\xi \quad 0<t<a\\ \delta=b\eta, & 0<\delta<b; \quad t=b\xi \quad 0<t<b\end{cases}.$$

Next, we multiply the above two equations of the system, respectively by $\frac{\sqrt{2\pi}}{4a\omega}\phi(au)$ and $\frac{\sqrt{2\pi}}{4b\omega}\psi(bu)$ and using the following substitutions

$$(4.17)\quad \begin{cases}\Phi(u)=\frac{\sqrt{2\pi}}{4a\omega}\phi(au) \quad \Psi(u)=\frac{\sqrt{2\pi}}{4b\omega}\psi(bu)\\ c=\frac{b}{a} \quad \lambda=\frac{x}{a} \quad H=\frac{h}{a} \quad \rho=\frac{r}{a} \quad \zeta=\frac{z}{a}\end{cases},$$

we obtain

$$(4.18)\quad \Phi(\xi)+c^2\sqrt{c}\sqrt{\xi}\int_0^1\sqrt{\eta}\Psi(s)K(\xi,\eta)d\eta=0,\quad \xi<1,$$

$$(4.19)\quad \Psi(\xi)+\frac{1}{\sqrt{c}}\sqrt{\xi}\int_0^1\sqrt{\eta}\Phi(\eta)L(\xi,\eta)d\eta=\xi,\quad \xi<1,$$

where

$$(4.20)\quad K(\xi,\eta)=-\int_0^\infty xe^{-xH}J_{\frac{3}{2}}(x\xi)J_{\frac{1}{2}}(xc\eta)dx$$

$$= -\frac{2}{\pi}\frac{1}{\sqrt{c\xi\eta}}\int_0^\infty e^{-xH}\sin(xc\eta)\Big[\frac{\sin(x\xi)}{x\xi} - \cos(x\xi)\Big]dx,$$

$$L(\xi,\eta) = \int_0^\infty xe^{-xH}J_{\frac{1}{2}}(xc\xi)J_{\frac{3}{2}}(x\eta)dx \tag{4.21}$$

$$= \frac{2}{\pi}\frac{1}{\sqrt{c\xi\eta}}\int_0^\infty e^{-xH}\sin(xc\xi)\Big[\frac{\sin(x\eta)}{x\eta} - \cos(x\eta)\Big]dx.$$

The indefinite integrals K and L can be evaluated in closed form given in (3:947:1-2), (3:948:2) and (3:893:1-2) from [27], and we obtain

$$K(\xi,\eta) = -\frac{1}{\pi\sqrt{\xi c\eta}}\Big[\frac{1}{2\xi}\log\frac{H^2+(c\eta+\xi)^2}{H^2+(c\eta-\xi)^2} - \Big(\frac{c\eta+\xi}{H^2+(c\eta+\xi)^2} + \frac{c\eta-\xi}{H^2+(c\eta+\xi)^2}\Big)\Big], \tag{4.22a}$$

$$L(\xi,\eta) = \frac{1}{\pi\sqrt{\eta c\xi}}\Big[\frac{1}{2\eta}\log\frac{H^2+(c\xi+\eta)^2}{H^2+(c\xi-\eta)^2} - \Big(\frac{c\xi+\eta}{H^2+(c\xi+\eta)^2} + \frac{c\xi-\eta}{H^2+(c\xi+\eta)^2}\Big)\Big]. \tag{4.22b}$$

5. Numerical results and discussion

As the kernels K and L are continuous on the interval $[0,1]$, the system of Fredholm integral equations can be solved by direct or iterative techniques [28]. The midpoint quadrature [29] is used to find the numerical solution for the system given by Eq. (4.18) and Eq. (4.19). We divide the interval $[0,1]$ into N equal subintervals so the midpoints are $u = u_m = \frac{2m-1}{2N}$, $s = u_n = \frac{2n-1}{2N}$ $m,n = 1,2\dots,N$ and introduce the following notations

$$\Phi(u_m) = \Phi_m, \qquad \Psi(u_m) = \Psi_m, \tag{5.1a}$$

$$K(u_m,u_n) = K_{mn}, \qquad L(u_m,u_n) = L_{mn}. \tag{5.1b}$$

Then considering the following transformations $\phi(a) = \frac{4a\omega}{\sqrt{2\pi}}\Phi_N$, $\psi(a) = \frac{4b\omega}{\sqrt{2\pi}}\Psi_N$, we obtain the following systems of finite algebraic equations in Φ_m and Ψ_m

$$\Phi_m + \frac{c^2\sqrt{c}}{N}\sqrt{u_m}\sum_{n=1}^{N}\sqrt{u_n}\Psi_n K_{mn} = 0, \quad m = 1,2,\dots,N, \tag{5.2}$$

$$\Psi_m + \frac{1}{N\sqrt{c}}\sqrt{u_m}\sum_{n=1}^{N}\sqrt{u_n}\Phi_n L_{mn} = u_m, \quad m = 1,2,\dots,N. \tag{5.3}$$

After solving the above system, the unknown coefficients Φ_m and Ψ_m can be obtained and then we get the numerical approximation of the unknown functions B_1, A_2, B_2 and A_3 given by Eq. (3.6a), Eq. (4.1a), Eq. (4.1b) and Eq. (3.6b)

$$B_1(x) = \frac{4a^2\omega}{N\sqrt{2\pi}}\sqrt{x}\sum_{m=1}^{N}\sqrt{u_m}[e^{-xH}c^2\sqrt{c}\Psi_m J_{\frac{1}{2}}(xcu_m) - \Phi_m J_{\frac{3}{2}}(xu_m)], \tag{5.4a}$$

$$A_2(x) = \frac{4a^2\omega}{N\sqrt{2\pi}}\sqrt{x}\sum_{m=1}^{N}\sqrt{u_m}\Phi_m J_{\frac{3}{2}}(xu_m), \tag{5.4b}$$

$$B_2(x) = e^{-xH}\frac{4b^2\sqrt{c}\omega}{N\sqrt{2\pi}}\sqrt{x}\sum_{m=1}^{N}\sqrt{u_m}\Psi_m J_{\frac{1}{2}}(xcu_m), \tag{5.4c}$$

$$A_3(x) = \frac{4a^2\omega}{N\sqrt{2\pi}}\sqrt{x}\sum_{m=1}^{N}\sqrt{u_m}[e^{xH}c^2\sqrt{c}\Psi_m J_{\frac{1}{2}}(xcu_m) + \Phi_m J_{\frac{3}{2}}(xu_m)]. \tag{5.4d}$$

5.1. Stress intensity factor. The stress intensity factors at the edge of the crack and at the rim of the disc are defined respectively by

$$K_{\mathrm{III}}^{a} = \lim_{r\to a^+}\sqrt{2\pi(r-a)}\tau_{\theta z}^{(2)}(r,z)|_{z=0}, \tag{5.5}$$

$$K_{\mathrm{III}}^{b} = \lim_{r\to b^-}\sqrt{2\pi(b-r)}\tau_{\theta z}^{(2)}(r,z)|_{z=h}. \tag{5.6}$$

On the plane $z=0$ for $r \geqslant a$, the expression of stress is given by

$$\tau_{\theta z}^{(2)}(r,0) = G\int_0^\infty \Big[-\lambda^{\frac{3}{2}}\int_0^a \sqrt{t}\phi(t)J_{\frac{3}{2}}(\lambda t)dt + e^{-\lambda h}\lambda^{\frac{3}{2}}\int_0^b \sqrt{t}\psi(t)J_{\frac{1}{2}}(\lambda t)dt\Big]J_1(\lambda r)d\lambda. \tag{5.7}$$

On the plane $z=h$, the expression of stress is given by

$$\tau_{\theta z}^{(2)}(r,h) = G\int_0^\infty \Big[-e^{-\lambda h}\lambda^{\frac{3}{2}}\int_0^a \sqrt{t}\phi(t)J_{\frac{3}{2}}(\lambda t)dt + \lambda^{\frac{3}{2}}\int_0^b \sqrt{t}\psi(t)J_{\frac{1}{2}}(\lambda t)dt\Big]J_1(\lambda r)d\lambda. \tag{5.8}$$

The second and the first parts of the integrals (5.7) and (5.8) respectively converge quickly, their limits as $r\to a$ and $r\to b$ automatically vanish, whereas the limits of the other two integrals are analyzed asymptotically as follows.

Using the relation

$$J_1(\lambda r) = -\frac{1}{\lambda}\frac{d}{dr}J_0(\lambda r), \tag{5.9}$$

we obtain

$$\tau_{\theta z}^{(2)}(r,0) = G\int_0^a \sqrt{t}\phi(t)dt\int_0^\infty F(\lambda,r)d\lambda + G\int_0^b \sqrt{t}\psi(t)dt\int_0^\infty e^{-\lambda h}\lambda^{\frac{3}{2}}J_{\frac{1}{2}}(\lambda t)J_1(\lambda r)d\lambda, \tag{5.10}$$

and

$$\tau_{\theta z}^{(2)}(r,h) = -G\int_0^a \sqrt{t}\phi(t)dt\int_0^\infty e^{-\lambda h}\lambda^{\frac{3}{2}}J_{\frac{3}{2}}(\lambda t)J_1(\lambda r)d\lambda \tag{5.11}$$

$$- G \int_0^b \sqrt{t}\psi(t)dt \int_0^\infty G(\lambda)d\lambda,$$

where

$$F(\lambda, r) = \lambda^{\frac{1}{2}} J_{\frac{3}{2}}(\lambda t) J_0(\lambda r), \tag{5.12}$$

$$G(\lambda, r) = \lambda^{\frac{1}{2}} J_{\frac{1}{2}}(\lambda t) J_0(\lambda r). \tag{5.13}$$

To calculate the limit of the integrals discussed above, we have to separate the terms obtained by numerical integration and those by application of asymptotic expansions of Bessel functions [30].

Once the value of λ becomes very large, we use the following asymptotic behavior of the Bessel function of the first kind

$$J_\nu(\lambda) \simeq \sqrt{\frac{2}{\lambda\pi}} \cos\Big(\lambda - \frac{\pi}{2}\nu - \frac{\pi}{4}\Big), \tag{5.14}$$

and then we get

$$J_{3/2}(\lambda t) \simeq \sqrt{\frac{2}{\lambda t\pi}} \cos(\lambda t - \pi) = -\sqrt{\frac{2}{\lambda t\pi}} \cos(\lambda t), \tag{5.15}$$

$$J_{1/2}(\lambda t) \simeq \sqrt{\frac{2}{\lambda t\pi}} \cos(\lambda t - \frac{\pi}{2}) = \sqrt{\frac{2}{\lambda t\pi}} \sin(\lambda t). \tag{5.16}$$

.

Then $F(\lambda, r)$ and $G(\lambda, r)$ are replaced, respectively, by $F'(\lambda, r)$ and $G'(\lambda, r)$ for large values of λ. This allows us to write

$$\int_0^\infty F(\lambda, r) = \int_0^\infty [F(\lambda, r) - F'(\lambda, r)]d\lambda + \int_0^\infty F'(\lambda, r)d\lambda, \tag{5.17}$$

$$\int_0^\infty G(\lambda, r) = \int_0^\infty [G(\lambda, r) - G'(\lambda, r)]d\lambda + \int_0^\infty G'(\lambda, r)d\lambda. \tag{5.18}$$

Since the first integrals in the above relations converge quickly, their limits as $r \longrightarrow a^+$ and $r \longrightarrow b^-$ vanish, whereas the limit of the second integrals gives the expression stress intensity factors.

We use the following integral formulas to replace the first infinite integrals respectively in the right part of Eq. (5.10) and Eq. (5.11)

$$\int_0^\infty \cos(\lambda t) J_0(\lambda r) d\lambda = \begin{cases} \frac{1}{\sqrt{r^2 - t^2}}, & r > t \\ 0, & r < t \end{cases}, \tag{5.19}$$

$$\int_0^\infty \sin(\lambda t) J_0(\lambda r) d\lambda = \begin{cases} 0, & r > t \\ \frac{1}{\sqrt{t^2 - r^2}}, & r < t \end{cases}, \tag{5.20}$$

and we obtain

$$\tau_{\theta z}^{(2)}(r, 0) = -\sqrt{\frac{2}{\pi}} G \frac{d}{dr} \int_0^a \frac{\phi(t)}{\sqrt{r^2 - t^2}} dt + R_1(r), \tag{5.21}$$

$$\tau_{\theta z}^{(2)}(r,h) = -\sqrt{\frac{2}{\pi}} G \frac{d}{dr} \int_0^b \frac{\psi(t)}{\sqrt{t^2 - r^2}} dt + R_2(r), \tag{5.22}$$

where

$$R_1(r) = G \int_0^b \sqrt{t} \psi(t) dt \int_0^\infty e^{-\lambda h} \lambda^{\frac{3}{2}} J_{\frac{1}{2}}(\lambda t) J_1(\lambda r) d\lambda, \tag{5.23}$$

$$R_2(r) = -G \int_0^a \sqrt{t} \phi(t) dt \int_0^\infty e^{-\lambda h} \lambda^{\frac{3}{2}} J_{\frac{3}{2}}(\lambda t) J_1(\lambda r) d\lambda. \tag{5.24}$$

Now integrating by parts, we get

$$\tau_{\theta z}^{(2)}(r,0) = G\sqrt{\frac{2}{\pi}} \left[\frac{a\phi(a)}{r\sqrt{r^2 - a^2}} - \int_0^a \frac{t\phi'(t)}{r\sqrt{r^2 - t^2}} dt \right] + R_1(r). \tag{5.25}$$

We note that the infinite integrals in the preceding expressions are convergent throughout the medium except at the singular points $r \to a^+$ which occupy the crack boundary.

$$\tau_{\theta z}^{(2)}(r,h) = G\sqrt{\frac{2}{\pi}} \left[\frac{b\psi(b)}{r\sqrt{b^2 - r^2}} - \int_r^b \frac{1}{r} \frac{t\psi'(t)}{\sqrt{t^2 - r^2}} dt \right] + R_2(r). \tag{5.26}$$

In this case, the Equation (5.26) shows that $\tau_{\theta z}^{(2)}(r,h)$ is $0(r)$ as $r \to 0$ and the integral is bonded as $r \to b^-$. As a result we obtain a square root singularity at $r = b$ and the constant $\psi(b)$ is the measure of the strength of singularity in the vicinity of the rigid inclusion.

The stress intensity factor at the edge of the rigid inclusion may be calculated as

$$K_{\mathrm{III}}^b = \lim_{r \to b^-} \sqrt{2\pi(b-r)} \frac{G\sqrt{2}}{\sqrt{\pi}} \frac{b\psi(b)}{r\sqrt{b^2 - r^2}}. \tag{5.27}$$

By using the following transformations: $\phi(a) = \frac{4a\omega}{\sqrt{2\pi}} \Phi_N$, $\psi(a) = \frac{4b\omega}{\sqrt{2\pi}} \Psi_N$, we obtain

$$K_{\mathrm{III}}^a = \frac{4G\omega\sqrt{a}}{\sqrt{\pi}} \Phi_N, \tag{5.28}$$

$$K_{\mathrm{III}}^b = \frac{4G\omega\sqrt{b}}{\sqrt{\pi}} \Psi_N. \tag{5.29}$$

The effect of the distance between the crack and the rigid inclusion H on the stress intensity factor is also shown in Figure 2. The increase in the height H induces the decrease in the stress intensity factor for all values of a/b.

Figure 3 illustrates the variation of the normalized stress intensity factor K_{III}^b at the edge of the rigid inclusion defined by Eq. (5.29) versus a/b for $H = 1, 0.75, 0.5$ and 0.25. It can be seen that the stress intensity factor starts with the value $4/\sqrt{\pi}$, which is the stress intensity factor in the vinicity of the rigid inclusion ($a \longrightarrow 0$) for a rigid disc alone in the infinite medium (not cracked). Furthermore, it first increases and then decreases to a minimum value and finally increases to $4/\sqrt{\pi}$. In addition, the interaction between the inclusion and the crack is small for smaller

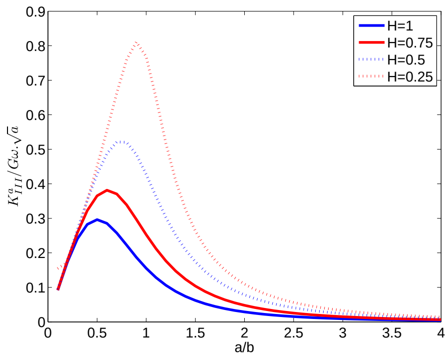

FIGURE 2. Variation of the normalized stress intensity factor at the edge of the crack K^a_{III} with a/b

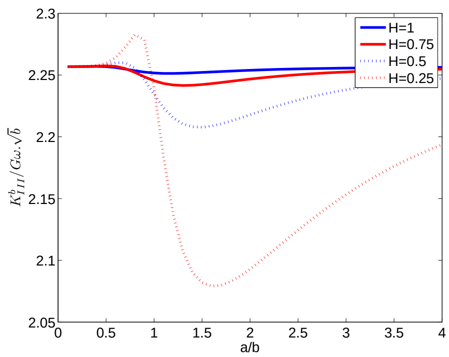

FIGURE 3. Variation of the normalized stress intensity factor at the edge of the rigid inclusion K^b_{III} with a/b

values of a/b and the values of the stress intensity factor are greater when the crack is closer to the disc.

5.2. Displacement and stress fields. By substituting Eqs. (5.4a)–(5.4d) into the expressions of the displacements and stresses Eqs. (3.4a)–(3.4f), we get the numerical results of displacements and stresses for the three regions.

The results for the variation of the normalized displacements $u_\theta^{(i)}(\rho,\zeta)/\omega a$ and the normalized stresses $\tau^{(i)}(\rho,\zeta)/\ G\omega a$ versus the normalized radius ρ are shown graphically in Figures 4 to 9 for the different values of the dimensionless axial distances $\zeta = z/a$. For each region, five different axial distances are selected as I ($\zeta = -H$; $-3H/4$; $-H/2$; $-H/4$; 0), II ($\zeta = 0$; $H/4$; $H/2$; $3H/4$;H), III ($\zeta = H$; $5H/4$; $3H/2$ $7H/4$;$2H$), with the particular values of the height $H = 1$ and the dimensionless disc sizes $c = 1$ and $c = 0.5$.

The variation of the normalized displacements is shown in Figures 4 to 6. We notice that the displacements in the three regions increase at first, reach maximum values at $\rho = c$ in regions 2 and 3 and then decrease out of the disc band with increasing ρ.

The distribution of the shear stresses in the elastic medium is also discussed and shown in Figures 7 to 9. It is concluded that the magnitude of the stress in the first region is lower than in the other three and that the stress are initially rises, attains its maximum values and with the increase in the value of ρ the stress goes on to decrease.

5.3. The moment required to produce rotation of the rigid inclusion. The torque required to sustain the rotation of the disc can be computed by

$$T = 2\pi \int_0^b r^2 \tau_{\theta z}(r,h)dr. \tag{5.30}$$

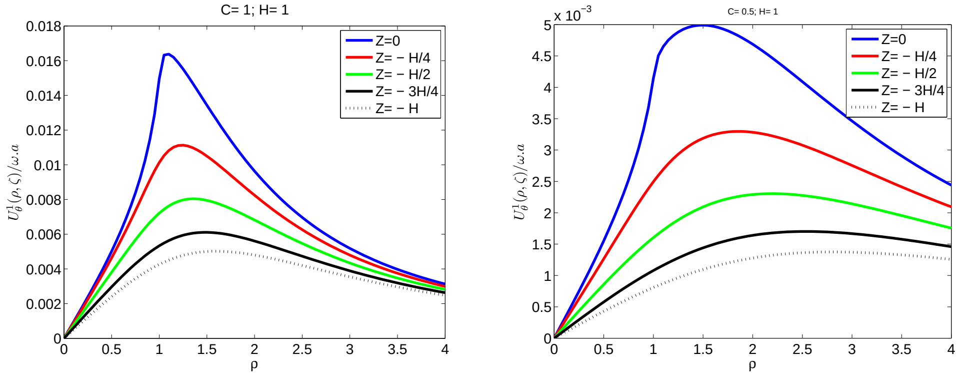

FIGURE 4. Tangential displacement u_θ^1 versus ρ for various ζ, $z \leqslant 0$

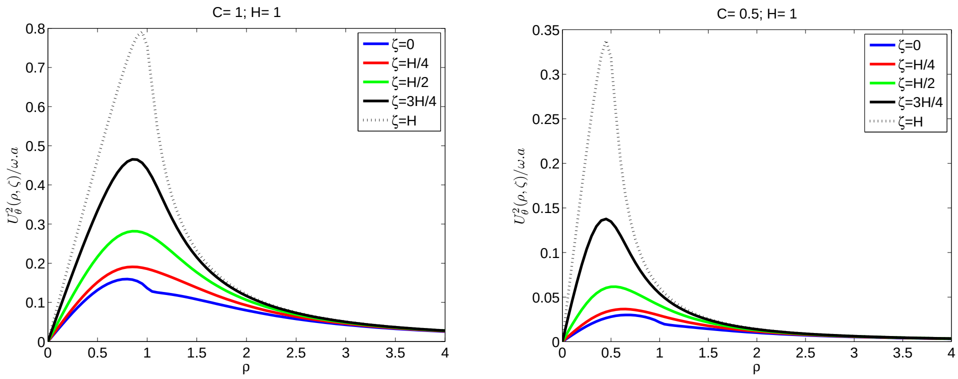

FIGURE 5. Tangential displacement u_θ^2 versus ρ for various ζ, $0 \leqslant z \leqslant h$

Using the relation

$$\int_0^b r^2 J_1(\lambda r) = \frac{b^2}{\lambda} J_2(\lambda b), \tag{5.31}$$

we get

$$T = 2\pi b^2 G \int_0^\infty [-A_2(\lambda)e^{-\lambda z} + B_2(\lambda)e^{\lambda z}] J_2(\lambda b) d\lambda. \tag{5.32}$$

Since here the moment is applied only to the rigid inclusion, the integrand is expressed in terms of $\psi(t)$. Substituting the values of $A_2(\lambda)$ and $B_2(\lambda)$ from Equations (4.1a) and (4.1b) into Equation (5.32) and using the asymptotic behavior of the Bessel function of the first kind $J_{\frac{1}{2}}$ we find that

$$T = 2\sqrt{2\pi} b^2 G \int_0^b \psi(t) dt \int_0^\infty \sin(\lambda t) J_2(\lambda b) d\lambda. \tag{5.33}$$

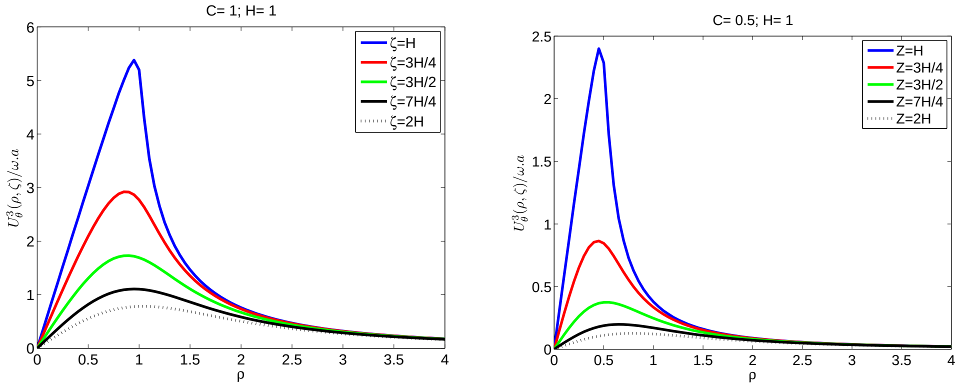

FIGURE 6. Tangential displacement u_θ^3 versus ρ for various ζ, $z \geqslant h$

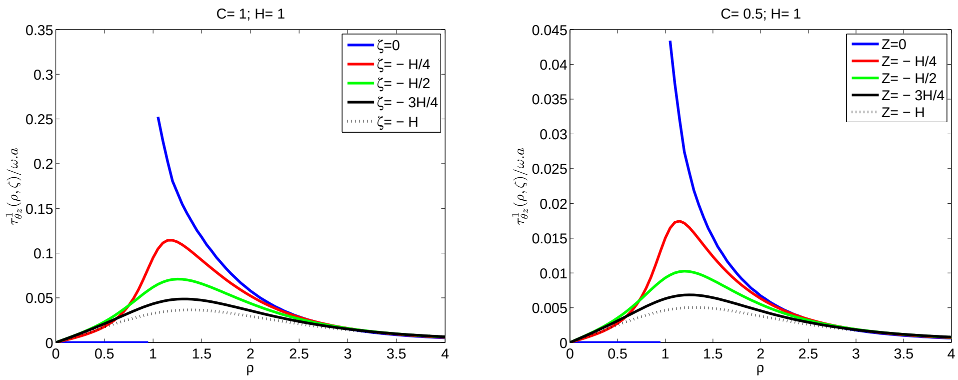

FIGURE 7. Shear stress $\tau_{\theta z}^1$ versus ρ for various ζ, $z \leqslant 0$

Taking into account the relation

$$\int_0^\infty J_2(\lambda b)\sin(\lambda t)dt = \frac{2t}{b^2}, \tag{5.34}$$

we obtain the moment applied to the inclusion

$$T = 4\sqrt{2\pi}G\int_0^b t\psi(t)dt. \tag{5.35}$$

By using the following transformations $t = bu$ and $\psi(bu) = \frac{4b\omega}{\sqrt{2\pi}}\Psi_u$, we get

$$T = 16\omega b^3 G\int_0^1 u\Psi(u)du. \tag{5.36}$$

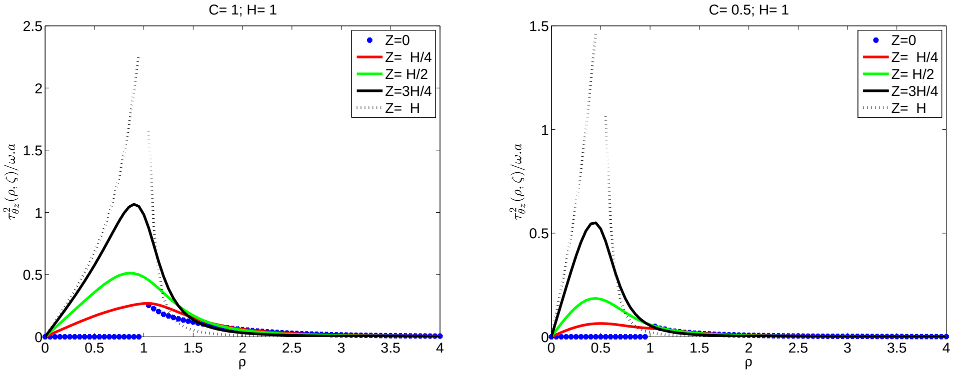

FIGURE 8. Shear stress $\tau^2_{\theta z}$ versus ρ for various ζ, $0 \leqslant z \leqslant h$

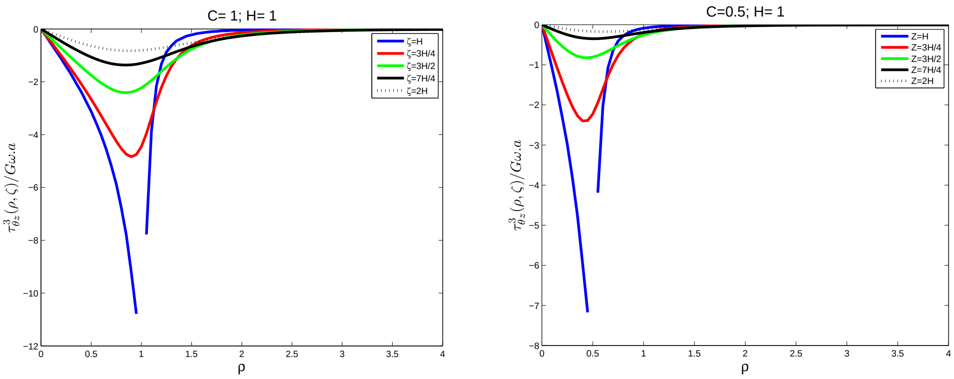

FIGURE 9. Shear stress $\tau^3_{\theta z}$ versus ρ for various ζ, $z \geqslant h$

The moment required to perform the rotation ω, when the medium contains no cracks and no inclusions can be formulated as [5–7, 24]

$$T_0 = \frac{16G\omega b^3}{3}.$$

Using the last relation, we find the dimensionless torque on the rigid disc

$$\frac{T}{T_0} = 3\int_0^1 u\Psi(u)du. \tag{5.37}$$

Equation (5.37) can be evaluated numerically. The moment is shown in Figure 10 as a function of the crack size. For this problem of pure shear, the moment increases with a/b, reaches its maximum and then decreases to a stable value.

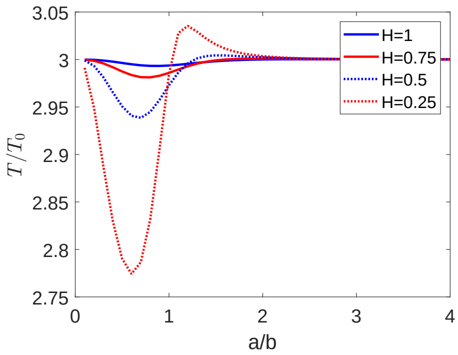

FIGURE 10. Variation of T/T_0 versus a/b for different H

6. Conclusion

In this study, the axisymmetric torsion problem of a circular rigid inclusion embedded in the interior of a homogeneous elastic material is analytically addressed. The medium is weakened by a penny-shaped crack located parallel to the plane of the inclusion. Using the Hankel integral transformation method, the doubly mixed boundary value problem is reduced to a system of dual integral equations, which are transformed to a Fredholm integral equations system of the second kind. The presented graphs show the variation of the displacements, the stresses in the three regions and the stress intensity factor at the edge of the crack and at the rim of the inclusion for some dimensionless parameters. The numerical results show that the discontinuities around the crack and the inclusion cause a large increase in the stresses which decay with distance from the loaded disc. Furthermore, we can observe the dependence of the stress intensity factor on the disc size and the distance between the crack and the rigid inclusion.

Acknowledgments. The Laboratoire de Génie Mécanique et Développement (LGMD) of Ecole Nationale Polytechnique (ENP) of Algiers is gratefully acknowledged for the resources and support.

References

1. A. P. S. Selvadurai, *Some annular disc inclusion problems in elasticity*, lnt. J. Solids. Struct. **20** (1984), 129–139.
2. A. P. S. Selvadurai, *Approximations for the low frequency response of a rigid plate embedded in an infinite space*, Soil Dynamics and Earthquake Engineering **2** (1983), 79–83.
3. A. P. S. Selvadurai, *Asymmetric displacements of a rigid disc inclusion embedded in a transversely isotropic elastic medium of infinite extent*, Int. J. Sci. **18** (1980), 979–986.
4. A. P. S. Selvadurai, *Rotary oscillations of a rigid disc inclusion embedded in an isotropic elastic infinite space*, Int. J. Solids Struct. **17** (1981), 493–498.
5. E. Reissner, H. F. Sagoci, *Forced torsion oscillation of an half-space I*, Int. J. Appl. Phys. **15** (1944), 652–654.
6. I. N. Sneddon, *Note on a boundary value problem of Reissner and Sagoci*, Int. J. Appl. Phys. **18** (1947), 130–132.

7. I. N. Sneddon, *The Reissner–Sagoci problem*, Glasg. Math. J. **7** (1966), 136–144.
8. S. Ufliand, *Torsion of an elastic layer*, Dokl. Akad. Nauk. SSSR **129** (1959), 997–999. (in Russian)
9. W. D. Collins, *The forced torsional oscillations of an elastic halfspace and an elastic stratum*, Proc. Lond. Math. Soc. **12** (1962), 226–244.
10. G. M. L. Gladwell, *The forced torsional vibration of an elastic stratum*, Int. J. Eng. Sci. **7** (1969), 1011–1024.
11. B. Noble, *The solution of Bessel function dual integral equations by a multiplying factor method*, Proc. Camb. Eng. Sci. **59** (1963), 351–362.
12. R. S. Dhaliwal, B. M. Singh, *Torsion of an elastic layer by two circular dies*, Int. J. Eng. Sci. **15** (1977), 171–175.
13. A. P. S. Selvadurai, *The statical Reissner–Sagoci problem for an internally loaded transversely isotropic halfspace*, Int. J. Eng. Sci. **20** (1982), 1365–1372.
14. R. Y. S. Pak, J. D. M. Saphores, *Torsion of a rigid disc in a half-space*, Int. J. Eng. Sci. **29** (1991), 1–12.
15. R. Bacci, S. Bennati, *An approximate explicit solution for the local torsion of an elastic layer*, Mech. Struct. Mach. **29** (1996), 21–38.
16. B. M. Danyluk, H. T. Vrbik, J. Rokne, R. S. Dhaliwal, *The Reissner–Sagoci problem for a non-homogeneous half-space with a surface constraint*, Meccanica **38** (2003), 453–465.
17. W. Guo-cai, C. J. Long-zhu, *Torsional oscillations of a rigid disc bonded to multilayered poroelastic medium*, J. Zhejiang Univ., Sci. **6(3)** (2005), 213–221.
18. M. Rahimian, A. K. Ghorbani-Tanha, M. Eskandari-Ghadi, *The Reissner–Sagoci problem for a transversely isotropic half-space*, Int. J. Numer. Anal. Methods Geomech. **30** (2006), 1063–1074.
19. H. Y. Yu, *Forced torsional oscillations of multilayered solids*, Int. J. Eng. Sci. **46** (2008), 250–259.
20. P. C. Pal, D. Mandal, B. Sen, *Torsional oscillations of a rigid disc embedded in a transversely isotropic elastic half-space*, Adv. Theor. Appl. Mech. **4** (2011), 177–188.
21. S. F. Ahmadi, M. Eskandari, *Rocking rotation of a rigid disk embedded in a transversely isotropic half-space*, Civil Engineering Infrastructures Journal **47** (2014), 125–138.
22. G. C. Sih, E. P. Chen, *Torsion of a laminar composite debonded over a penny-shaped area*, J. Franklin Inst. **293** (1972), 251–261.
23. R. D. Low, *On the torsion of elastic half space with embedded penny-shaped flaws*, J. Appl. Mech. **39** (1972), 786–790.
24. G. K. Dhawan, *On the torsion of elastic half-space with penny-shaped crack*, Def. Sci. J. **24** (1974), 15–22.
25. S. Basu, S. C. Mandal, *Impact of torsional load on a penny-shaped crack in an elastic layer sandwiched between two elastic half-space*, Int. J. Appl. Comput. Math. **2** (2016), 533–543.
26. L. Debnath, D. Bhatta, *Integral Transforms and Their Applications*, 2nd ed., Chapman and Hall/CRC, 2007.
27. G. K. Gradshteyn, I. M. Ryzhik, *Table of Integrals, Series, and Products*, 7th ed., Academic Press, New York, 2007.
28. F. K. Kythe, P. Puri, *Computational Methods for Linear Integral Equations*, Birkhäuser, Boston, 2002.
29. K. Atkinson, *The Numerical Solution of Integral Equations of the Second Kind*, Cambridge University Press, New York, 1997.
30. S. Chakraborty, D. S. Ray, A. Chakraborty, *A dynamical problem of Reissner-sogoci type for a non-homogeneous elastic half-space*, Indian J. Pure Appl. Math. **27**(8) (1996), 795–806.

МЕШОВИТИ ГРАНИЧНИ ПРОБЛЕМ ЕЛАСТИЧНЕ СРЕДИНЕ СА ЛОМОМ ПОД ТОРЗИЈОМ

Резиме. Овај рад има за циљ да истражи проблем пукотине у облику новчића у унутрашњости хомогеног еластичног материјала под осносиметричном торзијом кружном крутом инклузијом уграђеном у еластичну средину. Коришћењем Ханкеловог метода интегралне трансформације, мешовити гранични проблем се своди на систем дуалних интегралних једначина. Оне се своде на регуларан систем Фредхолмових интегралних једначина друге врсте које се затим решавају првилом квадратура. Нумерички резултати фактора померања, напрезања и интензитета напрезања су приказани графички у неким партикуларним случајевима разматраног проблема.

Department of Mechanical Engineering
Ecole Nationale Polytechnique
El-Harrach,
Algiers
Algeria
belkacem.kebli@g.enp.edu.dz

Department of Mechanical Engineering
Ecole Nationale Polytechnique
El-Harrach,
Algiers
Algeria
madanifateh1984@yahoo.com

(Received 23.09.2020.)
(Revised 17.06.2021.)
(Available online 23.11.2021.)